Received: 12 December 2020 | Accepted: 4 July 2021

DOI: 10.1111/mms.12852

ARTICLE

Marine Mammal Science

Glycopatterns of the foregut in the striped dolphin *Stenella coeruleoalba*, Meyen 1833 from the Mediterranean Sea

Roberto Carlucci[1] | Giulia Cipriano[1] | Carmelo Fanizza[2] | Tommaso Gerussi[3] | Rosalia Maglietta[4] | Antonio Petrella[5] | Guido Pietroluongo[3] | Pasquale Ricci[1] | Daniela Semeraro[1] | Marco Vito Guglielmi[1] | Giovanni Scillitani[1†] | Donatella Mentino[6†]

[1]Department of Biology, University of Bari Aldo Moro, Bari, Italy

[2]Jonian Dolphin Conservation, Taranto, Italy

[3]Archipelagos Institute of Marine Conservation, Pythagorio, Samos, Greece

[4]Institute of Intelligent Industrial Systems and Technologies for Advanced Manufacturing, National Research Council, Bari, Italy

[5]Istituto Zooprofilattico Sperimentale della Puglia e della Basilicata, Foggia, Italy

[6]Department of Biosciences, Biotechnologies and Biopharmaceutics, University of Bari Aldo Moro, Bari, Italy

Correspondence
Pasquale Ricci, Department of Biology, University of Bari, Via Edoardo Orabona, 4, 70125, Bari, Italy.
Email: pasquale.ricci@uniba.it

Funding information
Universita degli Studi di Bari Aldo Moro

Abstract

The glycopatterns of the glycans secreted by the mucosa of stomach and duodenal ampulla of the striped dolphin, *Stenella coeruleoalba* were studied by histochemical (Periodic acid-Schiff, Alcian Blue pH 2.5, High Iron Diamine) and lectin-binding (SBA, DBA, PNA, WGA, MAA-II, SNA, ConA, UEA-I, AAA, LTA) techniques. The stomach can be divided into four compartments: main stomach, two connecting chambers and pylorus. The pylorus is followed by the duodenal ampulla. Mucins are secreted by surface cells and intramucosal glands specific for each compartment. In the main stomach glands, neck cells were weakly sulphated, with prevailing glycosaminylated, glycosylated/mannosylated, and fucosylated residuals. Parietal and chief cells in general were scarcely reactive. In the connecting chambers glands, there were high levels of sulphation, glycosaminylation, glycosylation/mannosylation, and fucosylation, the latter with more complex patterns than those observed in the main stomach

Received: 12 December 2020 | Accepted: 4 July 2021

[†]Joint senior authors

glands. In the pyloric glands sulphated, glycosaminylated and fucosylated residuals decreased, whereas the opposite was observed for galactosyl/galactosaminylated residuals. Glycosylation patterns in the glands of the duodenal ampulla differed from those of the pyloric ones, with similar levels of sulphation, lower levels of galactosyl/galactosaminylation and glycosaminylation, and higher level of fucosylation. The results are compared with those available in literature.

KEYWORDS
cetacean stranding, foregut, histochemistry, lectin histochemistry, *Stenella coeruleoalba*

1 | INTRODUCTION

The stomach of Cetacea is plurilocular: it is subdivided into a series of compartments, the number of which varies among species and families (Cozzi et al., 2017; Harrison et al., 1970; Hosokawa & Kamiya, 1971; Langer, 1996; Mead, 2007; Slijper, 1962). Three main chambers are observed, e.g., the forestomach, the main stomach, and the pylorus. Each of these can be further subdivided and, in many species, there are some lesser chambers connecting the main stomach to the pylorus. In Odontoceti, the number of connecting chambers varies among species and up to 11 are observed in Ziphiidae (Mead, 2007). In addition, the duodenal ampulla can be present between the pylorus and the duodenum. In comparison to the anatomical studies, the histological analyses of the digestive tract, particularly the composition of the gastric secretions, are scarce (Cornaglia et al., 2000; Cozzi et al., 2017; Harrison et al., 1970; Hosokawa & Kamiya, 1971; Shimokawa et al., 2012; Smith, 1972; Tarpley et al., 1987; Yamasaki & Takahashi, 1971; Yamasaki et al., 1974). The mucosa of the forestomach is composed of a stratified squamous epithelium generally cornified and lacks glands. In the main stomach the mucosa is lined by a simple, cylindrical muciparous epithelium with gastric glands. These are of the tubular branched type and show three main cells involved in gastric juice production e.g., parietal, chief, and mucous neck cells. Sometimes, in the fore part of the main stomach a cardiac region with muciparous glands can be found. The parietal and the chief cells in the gastric glands secrete hydrochloric acid and pepsinogen, respectively, whereas neck cells are involved in the secretion of mucus, which forms a viscoelastic barrier lining the lumen of the stomach and has several functions, such as protection against physicochemical agents (including the gastric juice), lubrication to facilitate food passage, interactions with the microbiota (both symbiotes and pathogens), immunoregulation, coordination of cell proliferation, differentiation, and apoptosis (Bansil & Turner, 2018; Celli et al., 2009; Phillipson et al., 2008). The connecting chambers, the pylorus and the duodenal ampulla have a mucosa with a lining epithelium like that of the main stomach and muciparous glands.

One of the main components of mucus are mucins. These proteins are expressed by the Muc gene family and present several O-linked saccharidic chains whose patterns can change according to physiological and pathological conditions (Gomez-Santos et al., 2018; Wagner et al., 2018). Thus, knowledge about gastrointestinal mucin composition and variation is important in understanding physiological and pathological processes of the digestive tract. Lectin histochemistry is a useful tool in investigating mucin diversity in tissues (Brooks, 2017). In recent years, several studies appeared around gastric mucins characterization by lectin histochemistry in mammals (Fayed & Makita, 1997; Gomez-Santos et al., 2018; Lueth et al., 2005; Schumacher et al., 2004; Scillitani et al., 2007; Sommer et al., 2001).

By contrast, only one paper deals with gastric glycoconjugates in a cetacean species, the Pacific white-sided dolphin, *Lagenorhynchus obliquidens* (Shimokawa, et al., 2012).

The cetacean stranding monitoring system set in the Northern Ionian Sea (Carlucci et al., 2020) and Eastern Aegean Sea (Milani et al., 2017) (Mediterranean Sea) has offered the opportunity to examin carcasses of striped dolphins, *Stenella coeruleoalba* Meyen, 1833 and to collect samples to analyze the glycopatterns of their gastric mucosa and duodenal ampulla. This study increases knowledge about glycan variation and composition, which is almost unknown in cetacean species, representing a scientific reference for further comparative, functional, and pathological studies about *S. coeruleoalba*, which is the most abundant cetacean species in the Mediterranean Sea, although recently ranked as Vulnerable by the IUCN Red List (Braulik, 2019).

2 | MATERIAL AND METHODS

Five stranded females of *S. coeruleoalba* were collected on the coasts of the Gulf of Taranto (northern Ionian Sea) and Samos Island (eastern Aegean Sea) (Table 1). These areas host suitable habitats for the striped dolphin, which is widely distributed in offshore zones exploiting mainly benthopelagic prey (Carlucci et al., 2018a, b, 2021; Milani et al., 2018). The necropsy was carried out applying best practice on cetacean postmortem investigation and tissue sampling, collecting photo-video documentation and basic morphometric data (IJsseldijk et al., 2019). Stages of growth and physical maturity were estimated following Calzada & Aguilar (1996) and Calzada et al. (1997).

Samples of main stomach, connecting chambers, pylorus, and duodenal ampulla were removed from each individual and washed in phosphate-buffered saline (PBS) pH 7.4, 0.1 M, fixed in 10% neutral buffered formalin, dehydrated in a graded series of ethanol and embedded in paraffin wax. Sections were serially cut at 5 μm and mounted on slides for processing with conventional and lectin histochemistry.

2.1 | Conventional histochemistry

For conventional histochemistry, sections were rehydrated and stained with three methods: (1) Periodic-Acid Schiff (PAS) to demonstrate the presence of carbohydrates with 1,2 glycols; (2) Alcian Blue (AB) at pH 2.5, to demonstrate acidic glycans, both sulphated and sialylated; (3) high iron diamine (HID), to demonstrate acidic glycans with sulphated residuals. For each stain, counterstain with Mayer's hematoxylin (HE) was also performed. Protocol details have been reported previously (Petraccioli et al., 2013). All chemicals used in these procedures were from Sigma (St. Louis, MO). Photographs in bright light were taken by an Eclipse E600 photomicroscope equipped with a DMX1200 digital camera (Nikon Instruments SpA, Calenzano, Italy), keeping the same conditions for all the stains, tracts, and samples. Stain intensity was compared among tracts by computing optical density (OD) values from RGB

TABLE 1 Data recorded for the sampled individuals of *S. coeruleoalba* stranded in the Northern Ionian Sea (NI) and Eastern Aegean Sea (EA) (Mediterranean Sea).

Location	Sea	Date	GPS coordinates (decimal degrees)	Total length (cm)	Age class
Marina di Chiatona	NI	March 6, 2016	40.514489, 17.054043	150	Subadult
San Pietro in Bevagna	NI	November 5, 2018	40.304853, 17.680967	180	Adult
A. Konstantinos	EA	May 26, 2018	37.80621, 26.82541	200	Adult
A. Konstantinos	EA	March 1, 2019	37.808099, 26.808970	196	Adult
Karlovasi	EA	June 3, 2018	37.80262, 26.71240	201	Adult

photographs processed by the color deconvolution, a method that allows to separate color channels for the stain, the counterstain, and the background (Ruifrok & Johnston, 2001). For each stain and tract, three fields per individual were selected (size: 340 × 270 μm) and 10–20 secreting cells of each type having the best orientation were chosen for the analysis. Stain vectors for reference were created from single-stained slides as previously reported. Single cell ODs were computed from mean intensities of stain channels (Mastrodonato et al., 2017). Image analysis was performed with the ImageJ package (Rasband, 2016) implemented with the color deconvolution plugin (Landini et al., 2020).

OD values were analyzed by statistical methods to detect significant differences (Mastrodonato et al., 2017). Mean OD values from each staining and cell type were compared by one-way analysis of variance (ANOVA) followed by resampling through a 10,000-iteration bootstrap of the *F*-values. All tests for statistical significance were set at $p < .01$. Statistical computations were generated by the Real Statistics Resource Pack plugin for Excel (Release 4.3; Zaiontz, 2019).

For a verbal, semiquantitative evaluation of the stain intensity in the histochemical analyses, the range of OD values was divided into four intervals, labeled as follows: "weak," OD <1,000; "moderate," 1,000 < OD < 2,000; "strong," 2,000 < OD < 3,000; "intense," OD > 3,000.

2.2 | Lectin histochemistry

Binding experiments with 10 FITC-labelled lectins (SBA, DBA, PNA, WGA, MAA-II, SNA, ConA, UEA-I, AAA, LTA) from Vector Laboratories (Burlingame, CA) were performed to detect the main residuals in the oligosaccharidic chains. Details for the lectins employed, their concentrations, and sugar specificities are in Table 2. Lectin protocols followed manufacturer's instructions and were reported elsewhere (Scillitani et al., 2011). Sections were incubated in the dark for 1 hr at room temperature in the appropriate lectin solution in HEPES, then rinsed in the same buffer, and finally mounted in Fluoromount (Sigma-Aldrich) for observation. Controls for lectin labelling were performed as follows: (1) incubation with lectin-free HEPES; (2) incubation with lectin in presence of an inhibitory sugar (types and concentrations given in Table 2); (3) binding to secreting epithelia of the duodenum of the house mouse, *Mus musculus*, or Guinea-pig, *Cavia porcellus*, as well as to the egg extracellular matrix of the toad, *Bufo bufo*, the mucins

TABLE 2 Lectins used and their carbohydrate specificities. Abbreviations: Fuc, fucose; Gal, galactose; GalNac, N-acetylgalactosamine; GlcNac, N-acetylglucosamine; Glc, glucose; MαM, methyl-α-mannopyranoside; Man, mannose; Neu5Ac, N-acetylneuraminic acid; TACT, N, N′, N″-triacetylchitotriose.

Lectin	Source	Binding specificitiy	Lectin concentration (mg/ml)	Inhibitory sugar
SBA	*Glycine max*	GalNAc/Gal	0.02	0.2 M GalNAc
DBA	*Dolichos biflorus*	α-GalNAc	0.02	0.2 M GalNAc
PNA	*Arachis hypogaea*	Galβ1,3GalNAc	0.06	0.2 M Gal
WGA	*Triticum vulgaris*	(GlcNAcβ1,4)*n	0.02	0.01 M TACT
MAA-II	*Maackia amurensis*	Neu5Acα2,3Galβ1,3GalNAc	0.02	0.02 M Neu5Ac
SNA	*Sambucus nigra*	Neu5Acα2,6Gal/GalNAc	0.02	0.2 M Neu5Ac
Con A	*Canavalia ensiformis*	D-Man, D-Glc	0.05	0.1 M MαM
UEA-I	*Ulex europaeus*	Fucα1,2	0.10	0.2 M L-Fuc
AAA	*Aleuria aurantia*	Fucα1,6GlcNAcβNAsn Fucα1,3, Fucα1,4	0.10	0.2 M L-Fuc
LTA	*Tetragonolobus purpureus*	L-Fucα1,6GlcNAc L-Fucα1,2Galβ1,4[L-Fuc1,3] GlcNAcβ1,6R	0.10	0.2 M L-Fuc

of which have been previously demonstrated to be labeled by the tested lectins (Mentino et al., 2014; Scillitani & Mentino, 2015).

Except for lectins, all the chemicals used here were from Sigma-Aldrich (St. Louis, MO).

Images were captured under 495 nm fluorescence light using the same microscopic and photographic system used for conventional histochemistry, equipped with an epifluorescence device set.

For each binding experiment three fields per tract and specimen were considered and 10–20 cells for each type were selected for the analysis. For each cell, the corrected total cell fluorescence, CTFC (McCloy et al., 2014) was computed. Mean CTFC values were then processed for statistical comparisons among tracts and species by ANOVA with resampling, as previous, setting significant *p*-values at $p < .01$. Image analyses and statistical computations were conducted using the same software packages as above (Rasband, 2016; Zaiontz, 2019).

A verbal, semiquantitative evaluation of the lectin-binding intensity was obtained by dividing the range of CTFC values into four intervals, labeled as follows: "weak," CTFC <40,000; "moderate," 40,000 < CTFC <80,000; "strong," 80,000 < CTFC <120,000; "intense," CTFC >120,000.

3 | RESULTS

The main stomach of *S. coeruleoalba* presents a mucosa lined by surface cells of cubic or cylindrical shape (Figure 1a, b). Gastric glands open at the bottom of gastric pits, lined by foveolar cells similar to the surface cells. In the gastric gland three cell types are observed, i.e., chief, parietal, and neck (Figure 1c). Chief cells are cuboidal with cytoplasmic granules. Parietal cells are larger, ovoidal in shape and neck cells are small, polygonal and are scattered among the two previous described cell types. Surface, foveolar, and neck cells stain strongly with PAS (Figure 1a–c) and AB pH 2.5 (Figure 2a–c), whereas chief and parietal cells are weakly or not stained (Figures 1c and 2c). High Iron Diamine (HID) stain is strong in surface and foveolar cells and weak or absent in the neck, parietal, and chief cells. (Figure 3a–c). As far as lectin binding (Figures 4–8), surface, foveolar, and neck cells show similar binding patterns, with SBA (Figure 4a) and PNA (Figure 5a) reacting weakly or moderately, WGA (Figure 6a) and UEA-I (Figure 9a) reacting strongly or intensely, ConA (Figure 8a) moderately, and SNA (Figure 7a) and AAA (Figure 10a) weakly.

Chief and parietal cells in general stained weakly. DBA binds only to parietal cells (Figure 4a). MAA-II and LTA do not bind to any cell type (Figure 11).

Two consecutive connective chambers, indicated as oral and aboral, respectively, are found between the main stomach and the pylorus. The mucosa of both is lined by surface cells and several glands are observed, made by one type of secreting cells. Histochemical stains are similar, with surface and gland cells of both chambers staining strongly with PAS (Figure 1d, e), AB pH 2.5 (Figure 2d, e), and HID (Figure 3d, e). Gland cells in the aboral connecting chamber are particularly rich in HID-positive residuals (Figure 3e). Surface and glandular cells in the oral chamber bind intensely to WGA (Figure 6b), UEA-I (Figure 9b), and AAA (Figure 10b) and weak to moderately to SBA, PNA, SNA, and ConA (Figures 4b, 5b, 7b, 8b). Similar patterns were observed in the cells of the aboral chambers for SBA, PNA, WGA and AAA (Figures 4c, 5c, 6c, and 10c); SNA and ConA link with higher intensity (Figures 7c and 8c) and UEA-I binds only moderately to the surface cells (Figure 9c). DBA, MAA-II and LTA do not bind to any cell type in both the connecting chambers.

The pylorus has surface cells lining the lumen and mucous glands with a single type of secreting cells, like those of the connecting chambers (Figure 1f). Surface and gland cells are positive to PAS (Figure 1f) and AB pH 2.5 (Figure 2f), with the same intensity observed for mucous cells in the connecting chambers, whereas HID stain is moderate (Figure 3f). Positive cells are observed mainly in the base of the glands. Lectin-binding experiments show a strong to intense linking of SBA (Figure 4d) and WGA (Figure 6d) in both surface and glandular cells and of UEA-I in the glandular cells (Figure 9d). A weak binding is observed for PNA, SNA, and AAA (Figures 5d, 7d, 10d), whereas ConA stains moderately (Figure 8d). DBA, MAA-II, and LTA do not bind to any cell type.

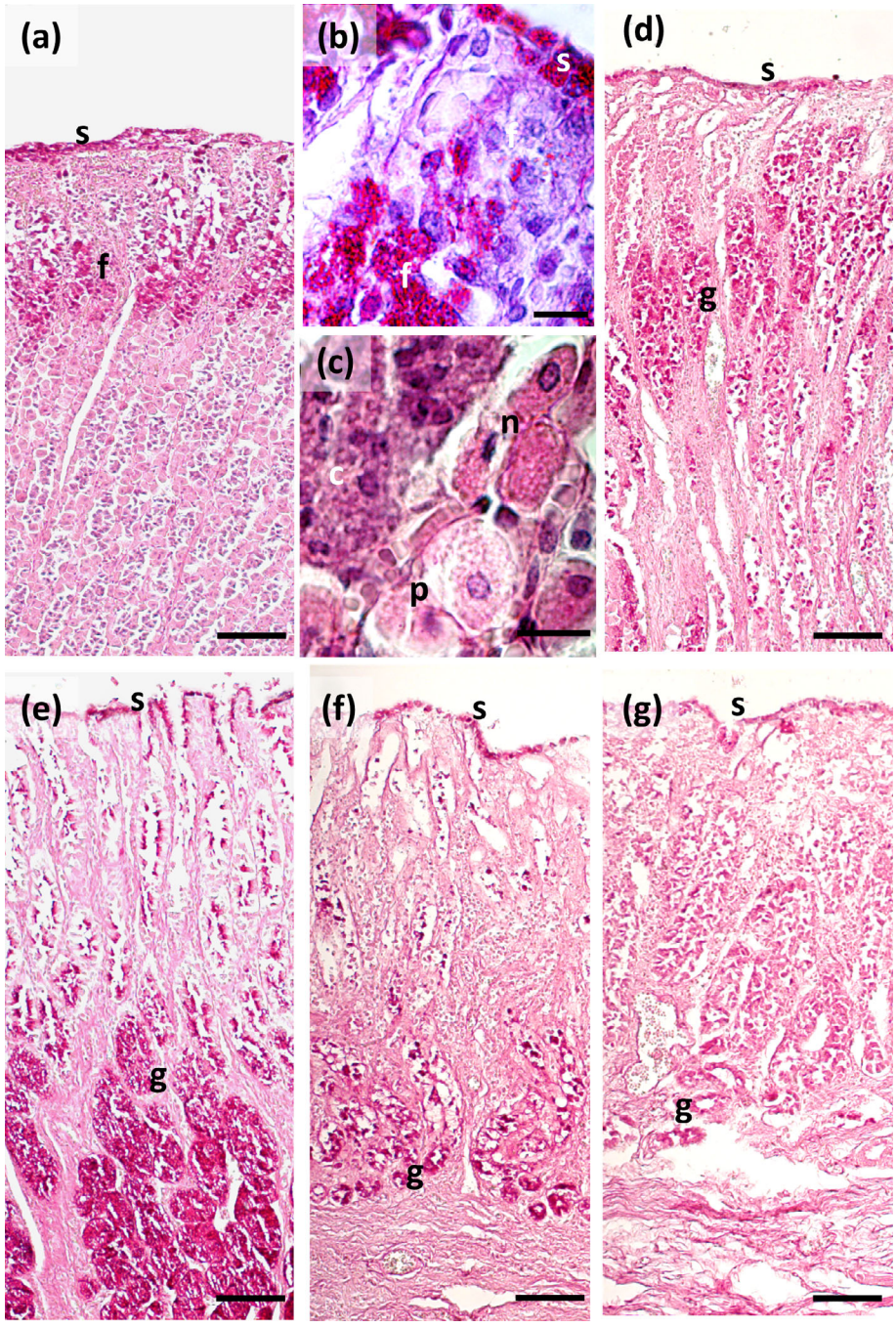

FIGURE 1 Sections of gastric mucosa of *Stenella coeruleoalba* stained with Periodic acid-Schiff (PAS)-hemalum. (a) Main stomach, general view. Surface and foveolar cells are strongly stained. (b) Main stomach; detail of a gastric pit with foveolar cells. (c) Main stomach; detail of gastric gland with neck, parietal, and chief cells. (d) Oral connecting chamber; surface and glandular cells are strongly stained. (e) Aboral connecting chamber; surface and glandular cells are strongly stained. (f) Pylorus; PAS-positive glandular cells are mostly in the glandular fundus. (g) Duodenal ampulla; PAS-positive glandular cells are mostly in the glandular fundus. Periodic acid-Schiff (PAS) - hemalum. Abbreviations: c, chief cell; f, foveolar cell; g, glandular cell; n, neck cell; p, parietal cell; s, surface cell. Scale bars: (a) 100 μm, (b) and (c) 10 μm, (d) to (g), 50 μm.

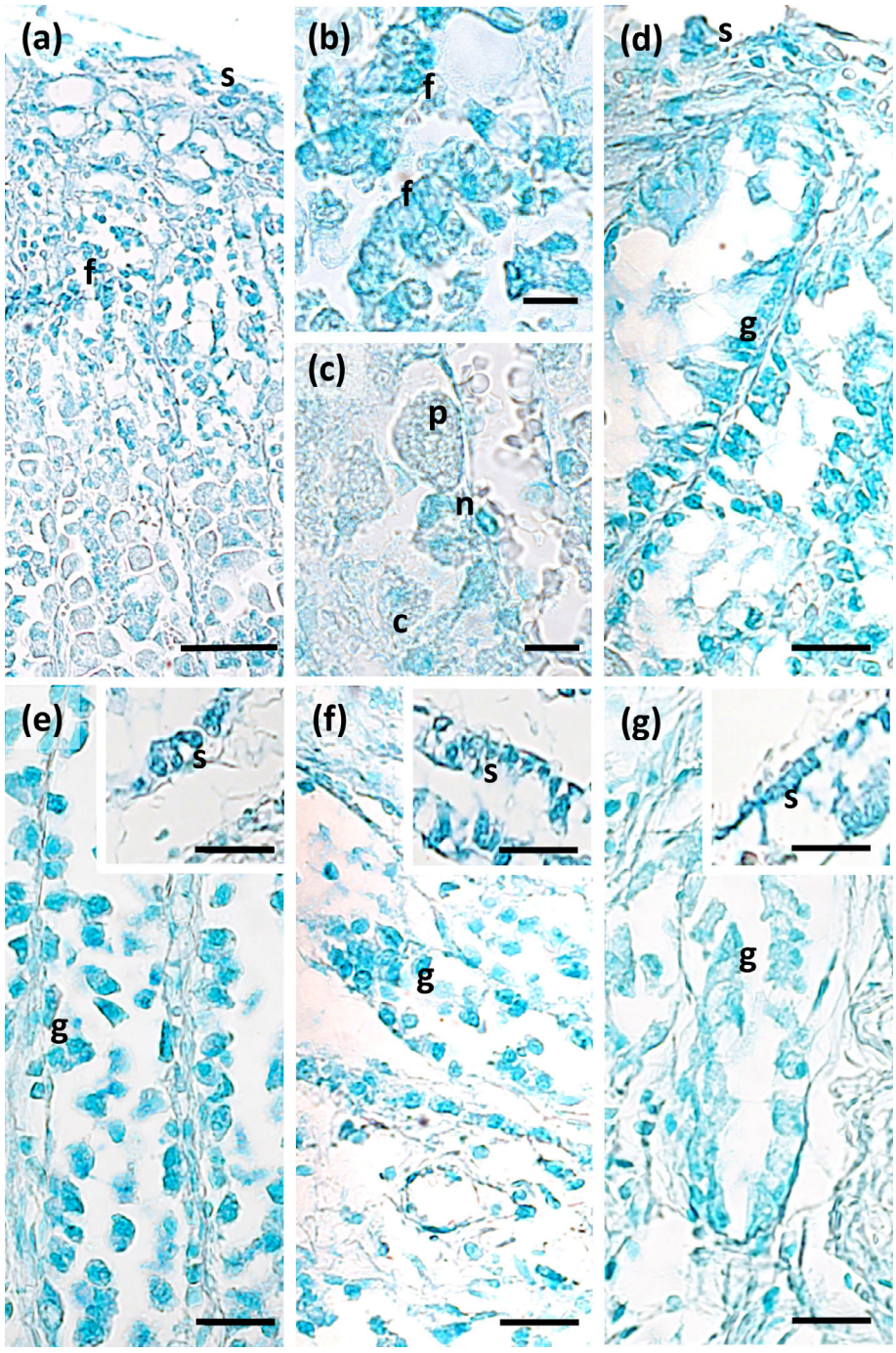

FIGURE 2 Sections of gastric mucosa of *Stenella coeruleoalba* stained with Alcian Blue (AB) pH 2.5. (a) Main stomach, general view. Surface and foveolar cells are strongly stained. (b) Main stomach; detail of a gastric pit with foveolar cells. (c) Main stomach; detail of gastric gland: only neck cells are stained. (d) Oral connecting chamber; surface and glandular cells are strongly stained. (e) Aboral connecting chamber; surface and glandular cells are strongly stained. (f) Pylorus; surface and glandular cells are strongly stained. (g) Duodenal ampulla; surface and glandular cells are strongly stained. Alcian Blue (AB), pH 2.5. Abbreviations: c, chief cell; f, foveolar cell; g, glandular cell; n, neck cell; p, parietal cell; s, surface cell. Scale bars: (a), 100 μm, (b) and (c) 10 μm, (d) to (g), 50 μm.

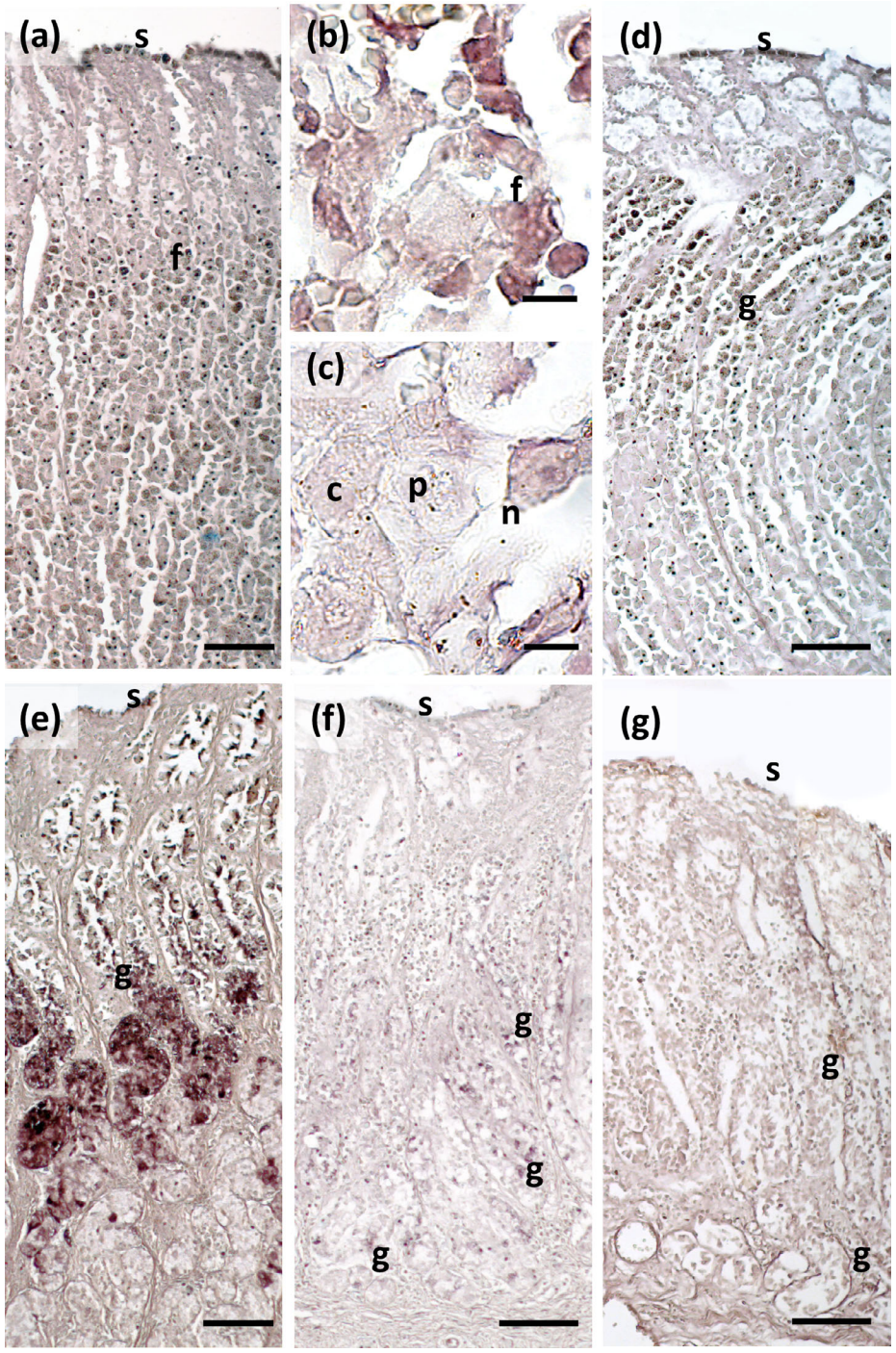

FIGURE 3 Sections of gastric mucosa of *Stenella coeruleoalba* stained with High-Iron Diamine (HID). (a) Main stomach, general view. Surface and foveolar cells are strongly stained. (b) Main stomach; detail of a gastric pit with foveolar cells. (c) Main stomach; detail of gastric gland: cells are weakly or not stained. (d) Oral connecting chamber; surface and glandular cells are strongly stained. (e) Aboral connecting chamber; surface and glandular cells are intensely stained. (f) Pylorus, few surface and glandular cells are moderately stained. (g) Duodenal ampulla; few surface and glandular cells are moderately stained. High-Iron Diamine (HID). Abbreviations: c, chief cell; f, foveolar cell; g, glandular cell; n, neck cell; p, parietal cell; s, surface cell. Scale bars: (a), 100 μm, (b) and (c) 10 μm, (d) to (g), 50 μm.

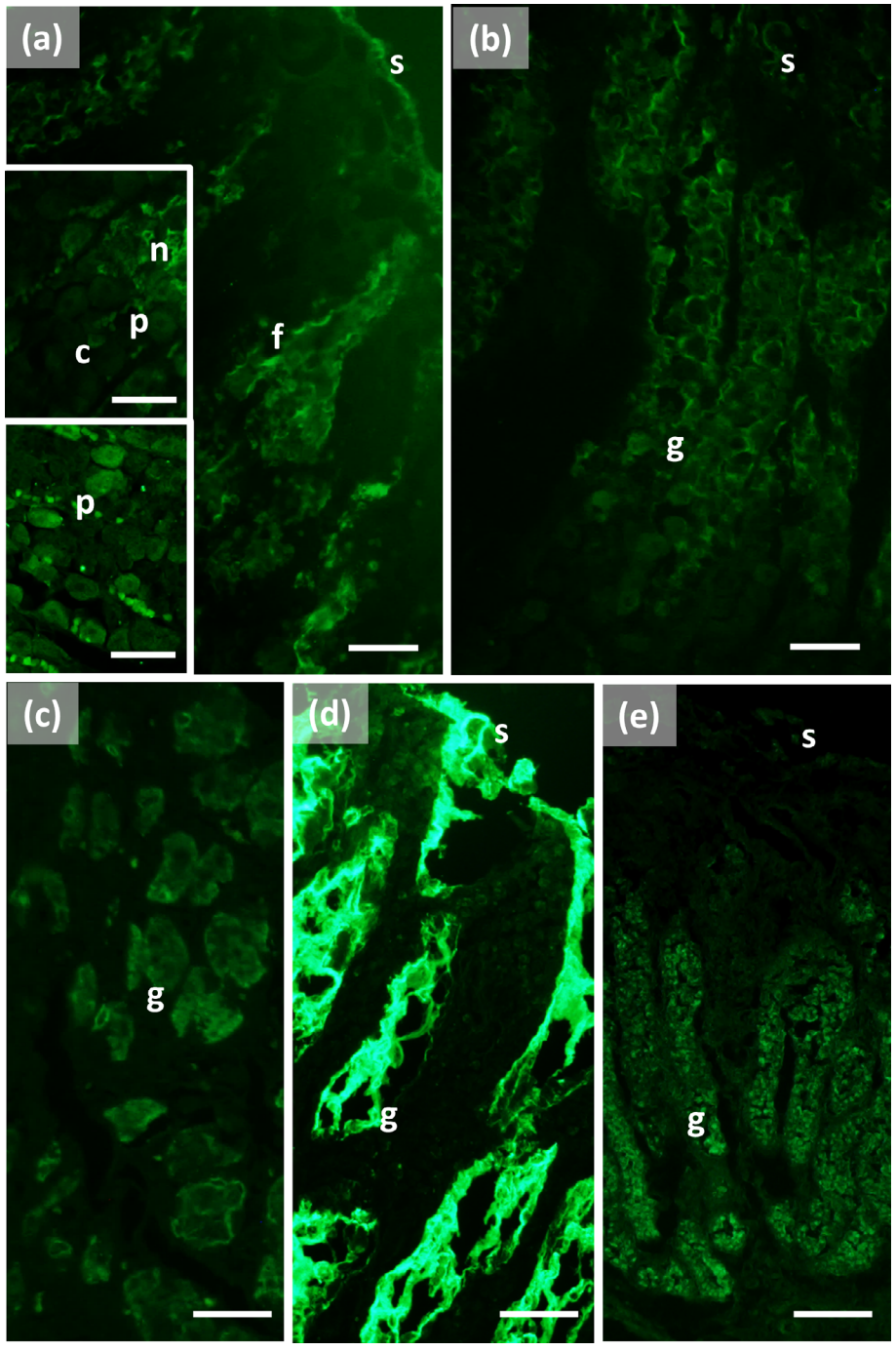

FIGURE 4 SBA- and DBA-binding to the cells of the gastric mucosa of *Stenella coeruleoalba*. (a) SBA. Main stomach; surface and foveolar cells are moderately stained. Insert, central left: SBA. Neck; chief, and parietal cells stain weakly. Insert, lower left: DBA. Only parietal cells bind to the lectin. (b) SBA. Oral connecting chamber; surface and glandular cells are weakly stained. (c) SBA. Aboral connecting chamber; glandular cells are weakly stained. (d) SBA. Pylorus; surface and glandular cells are strongly or intensely stained. (e) SBA. Duodenal ampulla; glandular cells are weakly or moderately stained. SBA-FITC and DBA-FITC. Abbreviations: c, chief cell; f, foveolar cell; g, glandular cell; n, neck cell; p, parietal cell; s, surface cell. Scale bars: 50 μm.

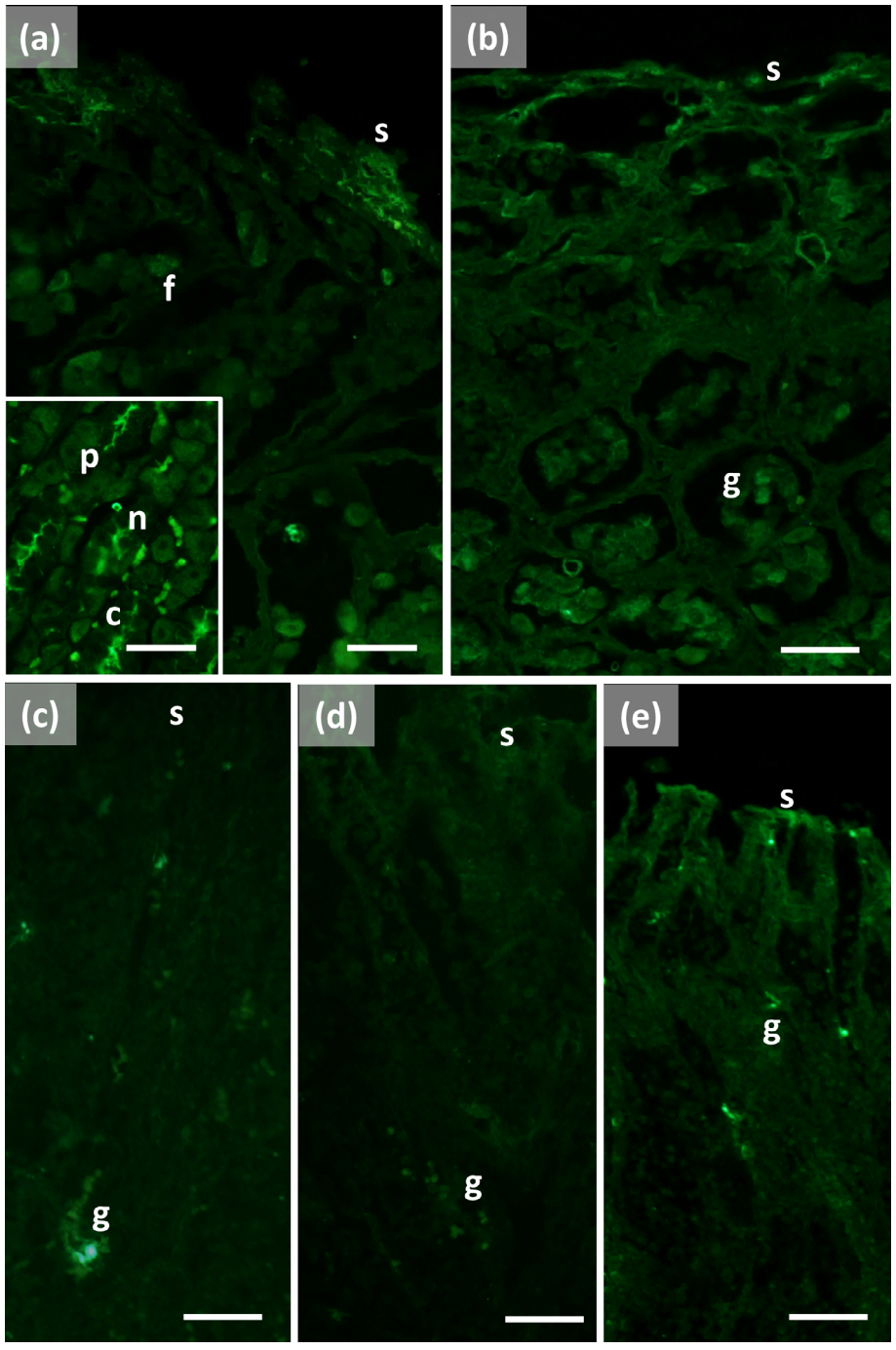

FIGURE 5 PNA-binding to the cells of the gastric mucosa of *Stenella coeruleoalba*. (a) Main stomach; surface and foveolar cells are moderately stained. Insert: neck cells stain weakly or moderately; chief and parietal cells weakly. (b) Oral connecting chamber; surface and glandular cells are weakly stained. (c) Aboral connecting chamber; surface and glandular cells are bound to lectin weakly or moderately. (d) Pylorus; surface and glandular cells are weakly or not stained. (e) Duodenal ampulla; few surface and glandular cells are weakly or moderately stained. PNA-FITC. Abbreviations: c, chief cell; f, foveolar cell; g, glandular cell; n, neck cell; p, parietal cell; s, surface cell. Scale bars: 50 μm.

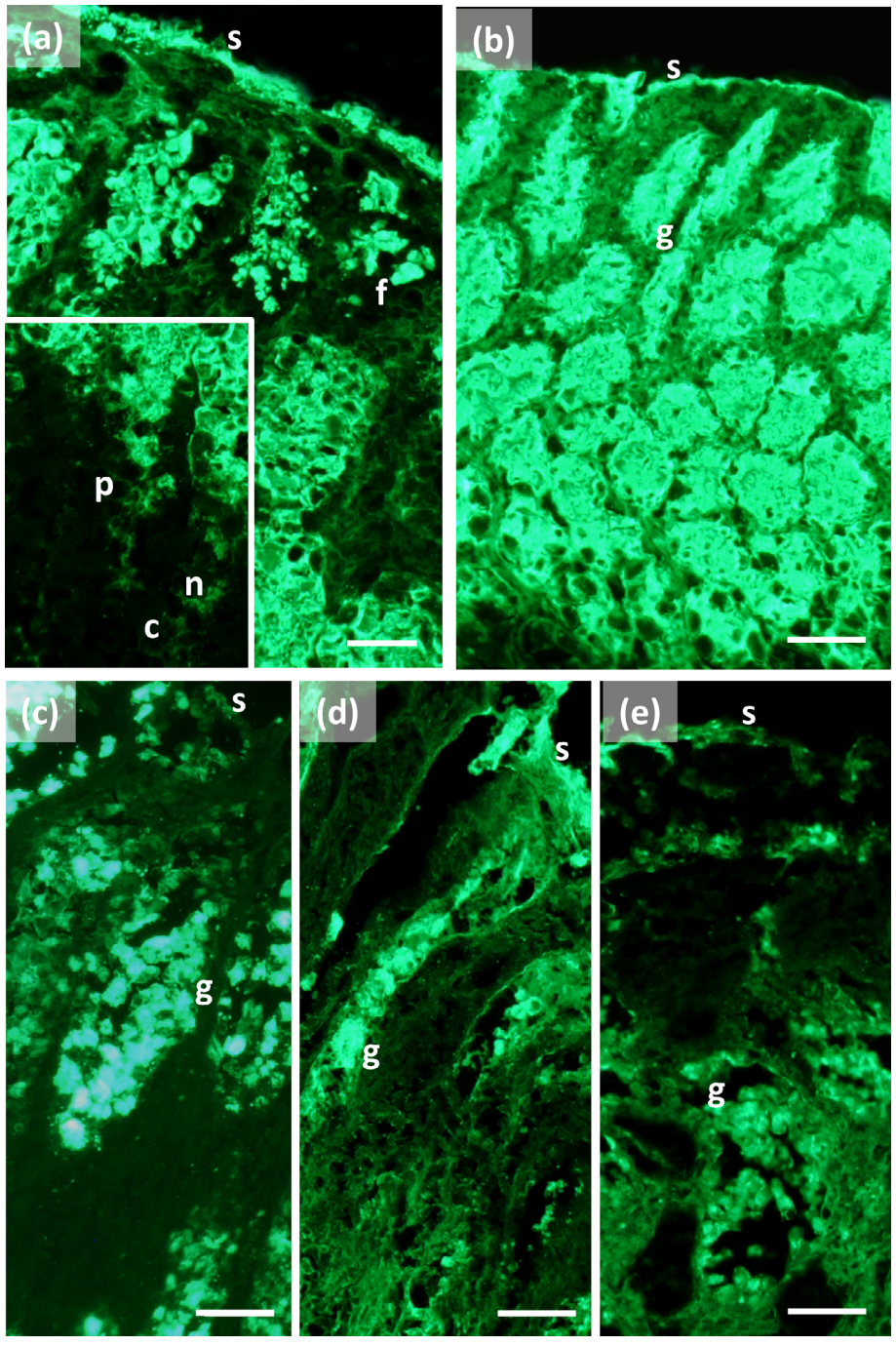

FIGURE 6 WGA-binding to the cells of the gastric mucosa of *Stenella coeruleoalba*. (a) Main stomach; surface and foveolar cells are intensely stained. Insert: neck cells are strongly stained and neck and parietal weakly stained. (b) Oral connecting chamber; surface and glandular cells are intensely stained. (c) Aboral connecting chamber; surface and glandular cells are intensely stained. (d) Pylorus; surface and glandular cells are intensely stained. (e) Duodenal ampulla; surface and glandular cells are strongly stained. WGA-FITC. Abbreviations: c, chief cell; f, foveolar cell; g, glandular cell; n, neck cell; p, parietal cell; s, surface cell. Scale bars: 50 μm.

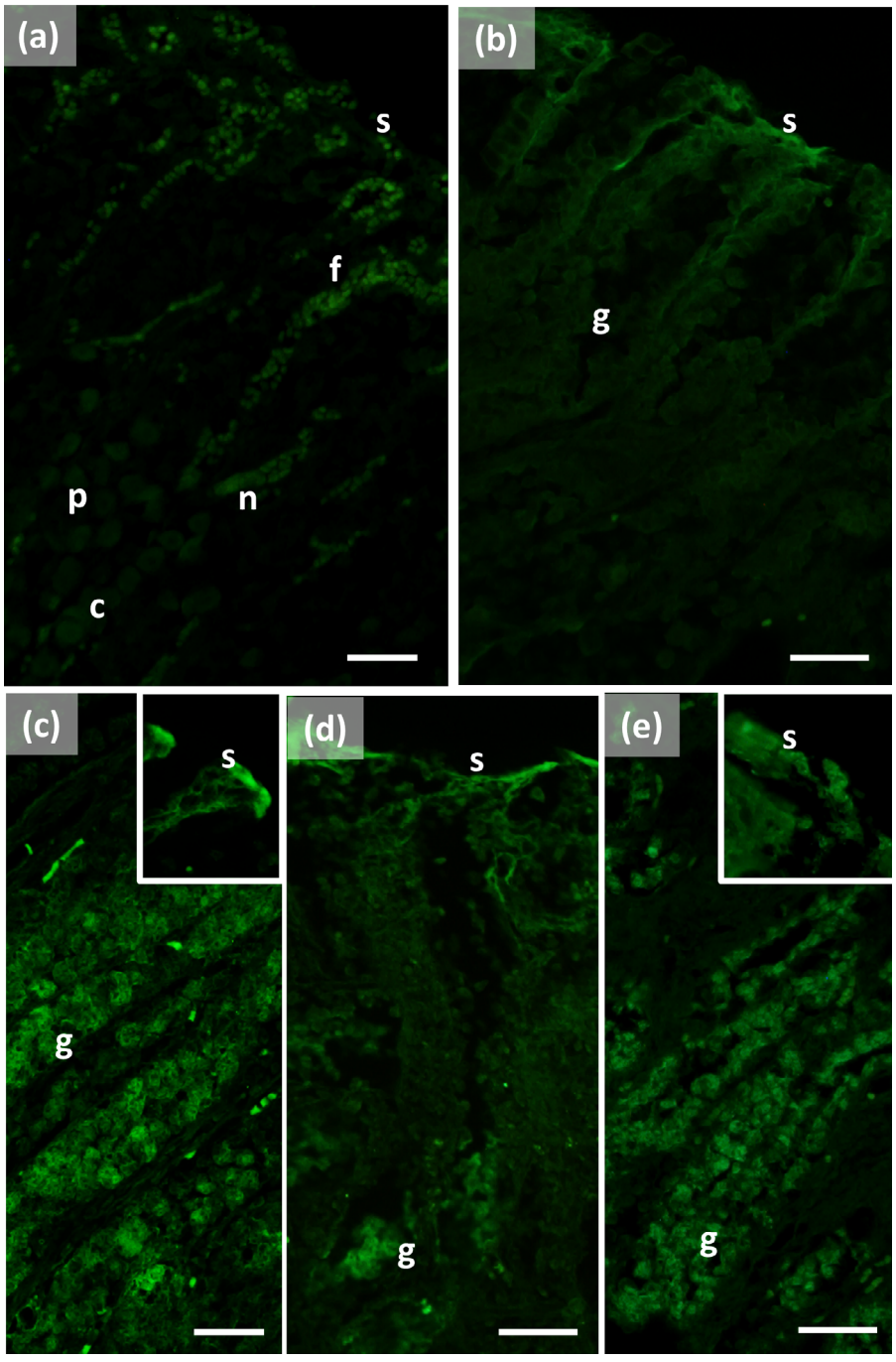

FIGURE 7 SNA-binding to the cells of the gastric mucosa of *Stenella coeruleoalba*. (a) Main stomach; surface, foveolar, and neck cells are weakly stained. (b) Oral connecting chamber; surface and glandular cells are weakly stained. (c) Aboral connecting chamber; surface (insert) and glandular cells are weakly or moderately stained. (d) Pylorus; surface, and glandular cells are weakly or moderately stained. (e) Duodenal ampulla; surface (insert) and glandular cells are weakly or moderately stained. SNA-FITC. Abbreviations: c, chief cell; f, foveolar cell; g, glandular cell; n, neck cell; p, parietal cell; s, surface cell. Scale bars: 50 μm.

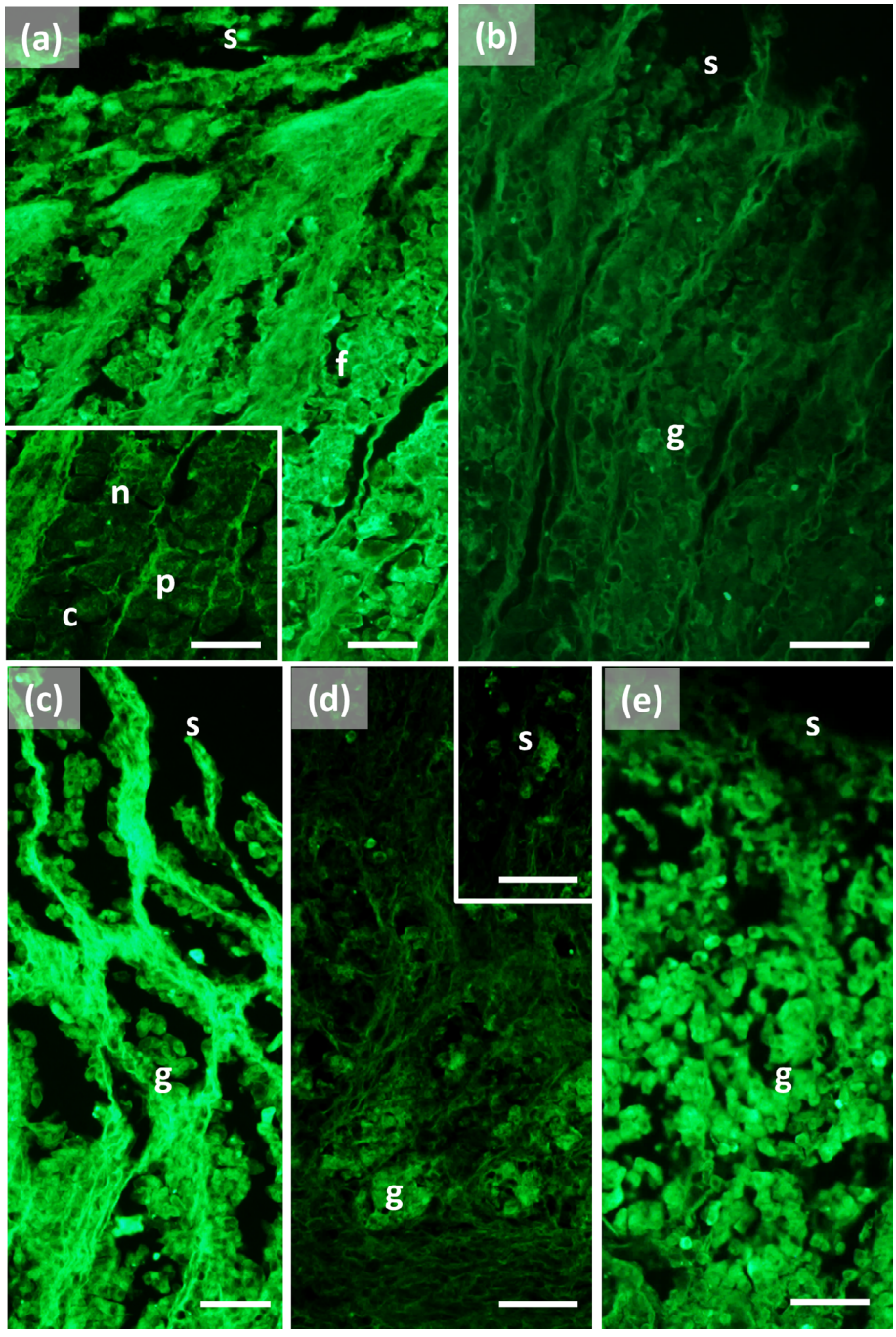

FIGURE 8 ConA-binding to the cells of the gastric mucosa of *Stenella coeruleoalba*. (a) Main stomach; surface and foveolar are strongly stained, and neck cells (insert) are moderately stained. (b) Oral connecting chamber; surface and glandular cells are moderately stained. (c) Aboral connecting chamber; surface and glandular cells are moderately to strongly stained. (d) Pylorus; surface (insert) and glandular cells are moderately stained. (e) Duodenal ampulla; surface cells are moderately stained and glandular cells are strongly stained. ConA-FITC. Abbreviations: c, chief cell; f, foveolar cell; g, glandular cell; n, neck cell; p, parietal cell; s, surface cell. Scale bars: 50 μm.

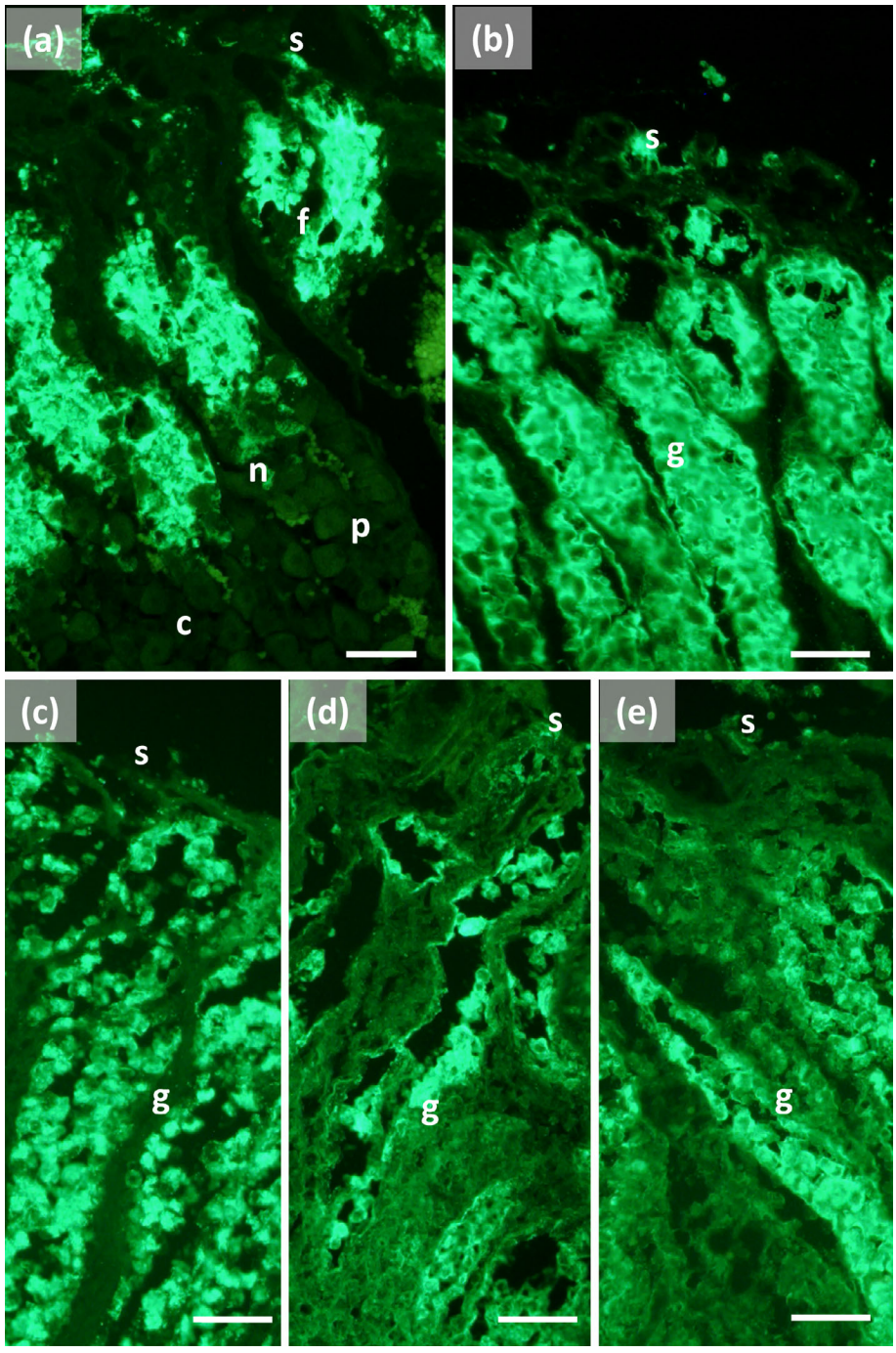

FIGURE 9 UEA-I-binding to the cells of the gastric mucosa of *Stenella coeruleoalba*. (a) Main stomach; surface, foveolar and neck cells are strongly or intensely stained, chief, and parietal are weakly stained. (b) Oral connecting chamber; surface and glandular cells are intensely stained. (c) Aboral connecting chamber; surface cells are moderately stained and glandular ones intensely stained. (d) Pylorus; surface cells are weakly stained and glandular cells are strongly stained (e) Duodenal ampulla; surface cells are weakly stained and glandular cells are strongly stained. UEA-I-FITC. Abbreviations: c, chief cell; f, foveolar cell; g, glandular cell; n, neck cell; p, parietal cell; s, surface cell. Scale bars: 50 μm.

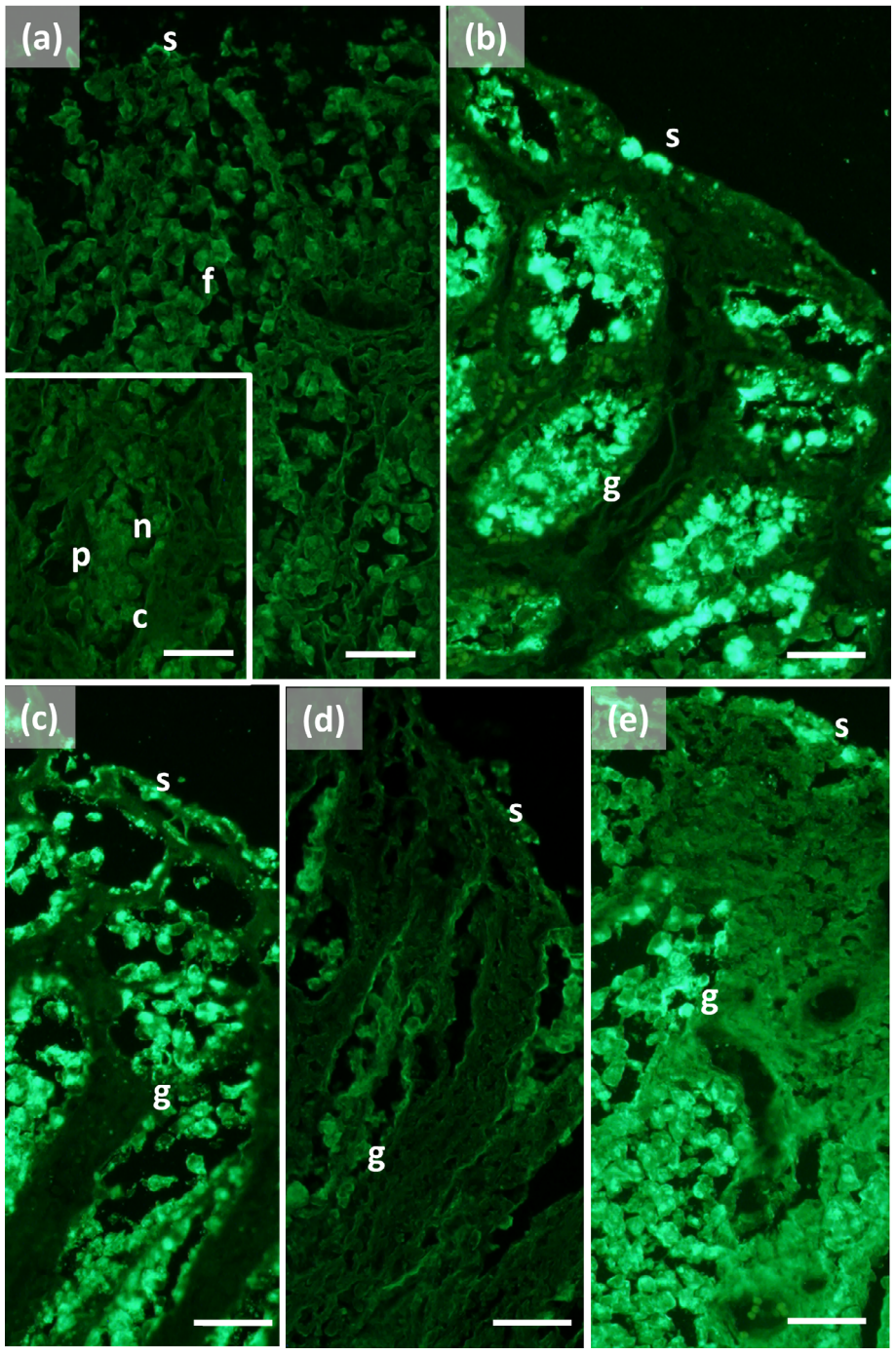

FIGURE 10 AAA-binding to the cells of the gastric mucosa of *Stenella coeruleoalba*. (a) Main stomach; surface and foveolar cells are weakly stained. Insert: neck, chief, and parietal cells are weakly stained. (b) Oral connecting chamber; surface and glandular cells are intensely stained. (c) Aboral connecting chamber; surface and glandular cells are intensely stained. (d) Pylorus; surface, and glandular cells are weakly stained. (e) Duodenal ampulla; surface and glandular cells are intensely stained. AAA-FITC. Abbreviations: c, chief cell; f, foveolar cell; g, glandular cell; n, neck cell; p, parietal cell; s, surface cell. Scale bars: 50 μm.

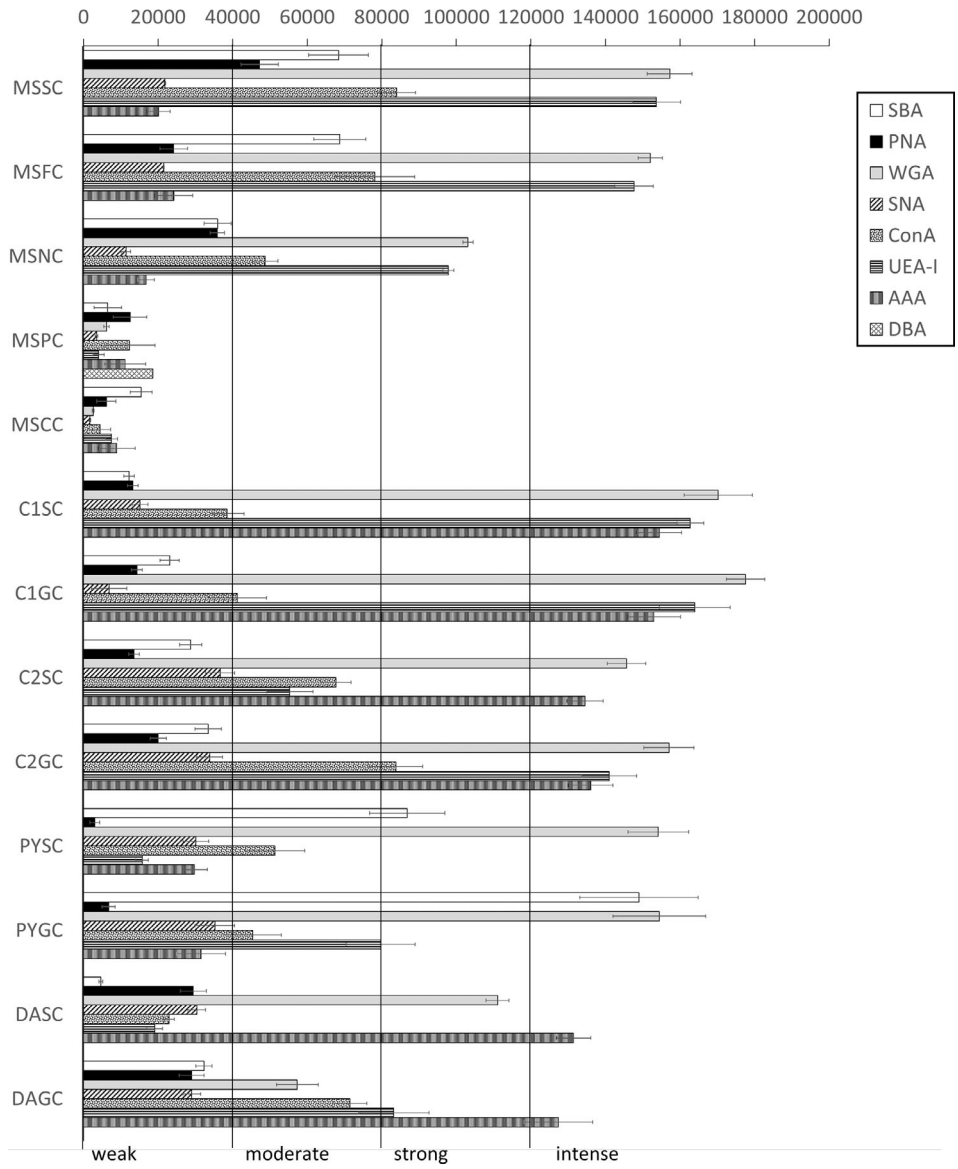

FIGURE 11 Plot of mean CTFC values and relative standard errors for the lectin-binding to the cells of the gastric mucosa of *Stenella coeruleoalba*. In the lower part there are the verbal evaluations for each interval in which the range of values was subdivided. Abbreviations: MSSC, main stomach surface cell; MSFC, main stomach foveolar cell; MSNC, main stomach neck cell; MSPC, main stomach parietal cell; MSCC, main stomach chief cell; C1SC, oral connecting chamber surface cell; C1GC, oral connecting chamber gland cell; C2SC, aboral connecting chamber surface cell; C2GC, aboral connecting chamber gland cell; PYSC, pylorus surface cell; PYGC, pylorus gland cell; DASC, duodenal ampulla surface cell; DAGC, duodenal ampulla gland cell.

The duodenal ampulla has surface and glandular cells like the previous tracts and villi are not observed. The histochemical staining patterns are similar to those of the pylorus (Figures 1g, 2g, and 3g). Lectin histochemical staining indicates strong to intense affinity of surface cells for WGA (Figure 6e) and AAA (Figure 10e), whereas glandular cells bind strongly or intensely to UEA-I (Figure 9e) and AAA (Figure 10e). SBA-linking is faintly visible in the surface cells and moderate in glandular cells (Figure 4e). PNA and SNA bind moderately to both surface and glandular cells

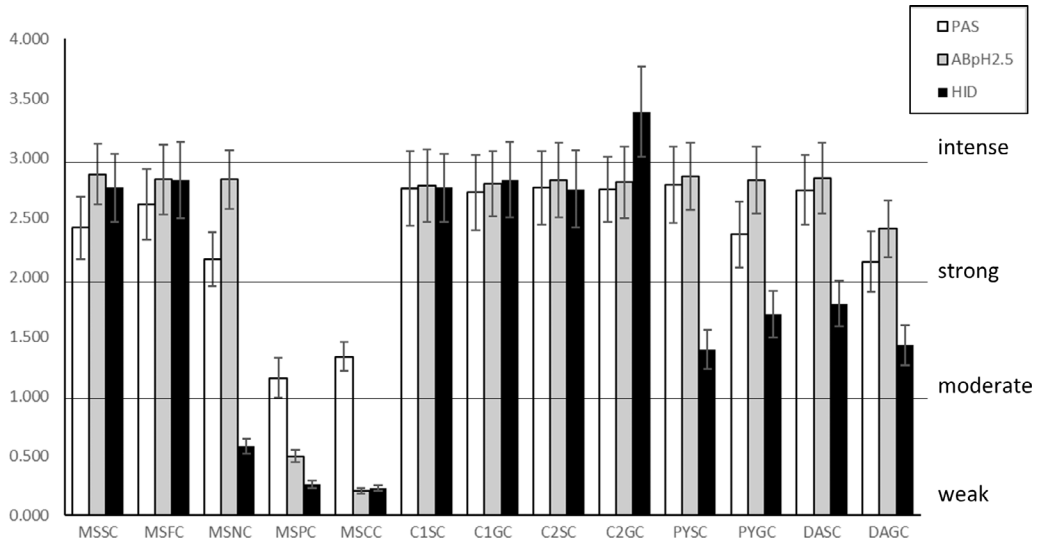

FIGURE 12 Plot of mean (± *SD*) optical density (OD) for the histochemical stains PAS (white), Alcian Blue pH 2.5 (gray), and HID (black) of tracts of the gastric mucosa of *S. coeruleoalba*. On the right there are the verbal evaluations for each interval in which the range of values was subdivided. Abbreviations: MSSC, main stomach surface cell; MSFC, main stomach foveolar cell; MSNC, main stomach neck cell; MSPC, main stomach parietal cell; MSCC, main stomach chief cell; C1SC, oral connecting chamber surface cell; C1GC, oral connecting chamber gland cell; C2SC, aboral connecting chamber surface cell; C2GC, aboral connecting chamber gland cell; PYSC, pylorus surface cell; PYGC, pylorus gland cell; DASC, duodenal ampulla surface cell; DAGC, duodenal ampulla gland cell.

(Figures 5e and 7e), whereas Con A binding is stronger in the glandular than in the surface cells (Figure 8e). WGA-linking is strong in the surface cells and moderate in the glandular ones (Figure 6e). DBA, MAA-II, and LTA do not bind to any cell type.

The mean values of OD computed for each cell type from histochemical stains are in Figure 12. PAS and AB pH 2.5 values are similar among the tracts, except for main stomach parietal and chief cells in which they are significantly lower, as confirmed by the ANOVA analysis (resulting in each test with $p < .0001$). HID values were also significantly lower in the pyloric and duodenal ampullar tracts in respect to the main stomach and connecting chambers.

The mean values of CTFC computed for each cell type from lectin-binding experiments are in Figure 11. In the chief and parietal cells of the main stomach low-intensity binding was generally observed. In surface, foveolar, and neck cells high intensities are observed for WGA and UEA-I. High values are also observed in surface and glandular cells of the subsequent tracts. AAA binding increases towards the connecting chambers, pylorus, and duodenal ampulla. High values of SBA characterize the pyloric cells. The low values in the chief and parietal cells and the higher values in the other glandular cells renders all the ANOVA test significant (resulting in each test with $p < .0001$).

All controls for lectin labeling were negative.

4 | DISCUSSION

The gastric mucosa of *S. coeruleoalba* has several types of secreting cells with variable distribution and secretion among compartments. Strong PAS-positivity in most cell types indicates secretion of glycoconjugates, mostly acidic, as indicated by AB- and HID-stains, as well as by WGA- and SNA-binding. Differences in lectin-binding reveals that glycosylation patterns differ among cell types. Glycan profiling was not considered for the esophagus and forestomach mucosae because they are not secreting tracts (Harrison et al., 1970).

Galactosylated and galactosaminylated residuals, as detected by PNA- and SBA-binding, respectively, are weakly or moderately represented, except for the pyloric gland cells, strongly stained by SBA. DBA also binds to galactosaminylated residuals, but only the parietal cells in the main stomach are positive to the lectin. This confirms the general affinity of this lectin to the HCl-secreting cells (both parietal and oxyticopeptic) in vertebrates (Liquori et al., 2005), probably due to residuals bound to the β-subunit of the integral glycoprotein H^+,K^+-ATPase in the tubule-vesicular system (Mastrodonato et al., 2009).

Both glycosaminylated and sialylated residuals are detected by the WGA lectin. Strong or intense binding indicates that these residuals are abundant along the stomach compartments. The SNA lectin detects sialylated residuals only: its lower affinity in respect to WGA suggests that the positivity of the latter is partly due to galactosaminylated residuals.

Mannosylated/glycosylated residuals are detected by ConA and they are moderately present in all the compartments. Fucosylated residuals link UEA-I (1,2-Fuc) and AAA (1,3-1,4- and 1,6-Fuc) lectins. Residuals fucosylated in 1,2 prevail in the main stomach, whereas those bound by AAA increase towards the connecting chambers. Glycans in the pyloric mucosa present a general lower fucosylation, increasing in the duodenal ampulla due to a raise in AAA-positive residuals.

A comparison of these results with the few available references on Odontoceti confirms that the mucosae of the various gastric tracts secrete sialosulphomucins, as revealed by AB-positivity at both pH 2.5 and 1.0 (Harrison et al., 1970; Shimokawa et al., 2012). The only available study about glycan profiling of mucins deals with the gastric mucosa of the Pacific white-sided dolphin, *Lagenorhynchus obliquidens* (Shimokawa et al., 2012). Similar to *S. coeruleoalba*, the mucins secreted by both the main stomach and the pylorus have galactosyl/galactosaminylated, glycosyl/glycosaminylated, mannosylated and fucosylated residuals. As far as the parietal and the chief cells of the gastric glands in the main stomach, in *L. obliquidens* there are neutral carbohydrates and glycan profiling is similar to the mucous cells. Shimokawa et al. (2012) attribute the stain of the parietal cells to the oligosaccharidic chains of the glycoproteins bound to the membranes of the tubule-vesicular system and the positivity of the chief cells to the pepsinogen granules. In *S. coeruleoalba* both parietal and chief cells resulted AB- and HID-negative, confirming the presence of neutral glycans, but they generally bind weakly to the lectins. These differences could be explained in terms of differences in the techniques used for the lectin-binding (we used FITC-labeled lectins instead of biotinylated lectins like Shimokawa et al. 2012 did) or by interspecific differences between the two distantly related species (McGowen, 2011).

Dolphins swallow their prey whole and salivary glands are absent or reduced (Cozzi et al., 2017), with the main mechanical and chemical treatments of food occurring in the stomach. The forestomach is involved in grinding and squeezing prey and has no secreting activity (Cozzi et al., 2017; Smith, 1972); the gastric juice can reflux from the main stomach and thus begin the chemical treatment, that takes place mostly in the main stomach (Smith, 1972). This is confirmed by the functional interpretation of results from this study. In fact, mucins in the main stomach are involved in the protection of the mucosa from mechanical insults, pathogens, oxidating agents, and gastric juice (Bansil & Turner, 2018). Acidic residuals like the sialylated and sulphated ones modulate most of these functions by forming a polyanionic barrier that protects the underlying cell layer. Other saccharidic residuals in the mucins probably coadiuvate in the protecting functions: as an example, glucosamine is known to prevent peptic ulcers (Santhosh et al., 2007), while fucose affects mucus viscosity and reduces bacterial motility (Becker & Lowe, 2003).

Posterior to the main stomach there are two connecting chambers with pyloric-like glands. The presence of valves suggest that they regulate the flow of chyme from the main stomach to the pylorus (Smith, 1972). Mucus secreted by the connecting chambers is rich in sulphates, in particular the aboral portion, and fucose links in more complex patterns than those of the main stomach (indicated by the strong binding of both AAA and UEA-I). Since both sulphates and fucose are involved in the regulation of the interactions with the microbiota (Ouwerkerk et al., 2013), we hypothesize that the connecting chambers could be important in protecting the posterior tracts from ingested pathogens.

The secretion of the pyloric glands differs from those of the connecting chambers. In the pyloric glands a higher amount of galactosaminylated residuals is observed in respect to the connecting chambers, whereas a lower amount of sulphated and fucosylated residuals is found. According to Smith (1972) in the harbor porpoise, *Phocoena phocoena*, the pylorus has the main function to adjust the pH of the chyme and regulate its passage to the duodenum by the pyloric sphincter. It is not clear whether galactosaminylated residuals could be involved in these functions, but the low amount of fucose and sulphates suggest that the pyloric mucus has the main function to lubricate the luminal surface for chyme passage.

The duodenal ampulla is regarded as the first tract of the small intestine, and it appears similar to the pylorus with the same type of mucous glands and lack of villi, but this could be a postmortem artifact (Cozzi et al., 2017). The composition of mucins anyway differs from those of the pyloric glands, with lower levels of galactosamine and higher fucosylation, maybe related to absorption and forming a barrier against bacteria (Mastrodonato et al., 2013). It is worthwhile noting that the duodenum of Cetacea lacks true Brunner's glands (Langer, 2017). However, Zhou & Li (1981) speculated that the lower part of the glands in the duodenal ampulla of the baiji, *Lipotes vexillifer*, could represent rudimentary Brunner's glands. In general, pyloric and Brunner's glands show very similar glycopatterns (Schumacher et al., 2004), but in *S. coeruleoalba* the differences we observed between the two gland types do not support the identification of the duodenal ampullar glands with Brunner's ones.

In conclusion, the present study showed that the mucin composition in the stomach of *S. coeruleoalba* varies among cells and compartments and that this is probably related to the different functions of mucus in the gastric chambers. Many aspects of functionality need clarification, requiring further research on a wide array of species to better understand mucin diversity and function in odontocetes.

ACKNOWLEDGMENT

Open Access Funding provided by Universita degli Studi di Bari Aldo Moro within the CRUI-CARE Agreement.

AUTHOR CONTRIBUTIONS

Roberto Carlucci: Conceptualization; investigation; project administration; writing - original draft; writing-review & editing. **Giulia Cipriano:** Investigation. **Carmelo Fanizza:** Conceptualization; funding acquisition; investigation; resources. **Tommaso Gerussi:** Investigation. **Rosalia Maglietta:** Investigation. **Antonio Petrella:** Investigation. **Guido Pietroluongo:** Funding acquisition; resources. **Pasquale Ricci:** Investigation. **Daniela Semeraro:** Formal analysis; investigation. **Marco Guglielmi:** Formal analysis. **Giovanni Scillitani:** Conceptualization; formal analysis; investigation; project administration; resources; writing - original draft; writing-review & editing. **Donatella Mentino:** Formal analysis; investigation; writing - original draft; writing-review & editing.

ORCID

Roberto Carlucci https://orcid.org/0000-0002-9287-6936
Guido Pietroluongo https://orcid.org/0000-0001-8578-6038
Pasquale Ricci https://orcid.org/0000-0003-1098-3824

REFERENCES

Bansil, R., & Turner, B. S. (2018). The biology of mucus: Composition, synthesis and organization. *Advanced Drug Delivery Reviews*, *124*, 3–15. https://doi.org/10.1016/j.addr.2017.09.023

Becker, D. J., & Lowe, J. B. (2003). Fucose: biosynthesis and biological function in mammals. *Glycobiology*, *13*(7), 41R–53R. https://doi.org/10.1093/glycob/cwg054

Braulik, G. (2019). *Stenella coeruleoalba*. *IUCN Red List of Threatened Species* 2019. https://doi.org/10.2305/IUCN.UK.2019-1.RLTS.T20731A50374282.en

Brooks, S. A. (2017). Lectin histochemistry: historical perspectives, state of the art, and the future. In C. Pellicciari & M. Biggiogera (Eds.), *Histochemistry of single molecules* (Vol. 1560, pp. 93–107). Humana Press. https://doi.org/10.1007/978-1-4939-6788-9_6

Calzada, N., & Aguilar, A. (1996). Flipper development in the Mediterranean striped dolphin (*Stenella coeruleoalba*). *Anatomical Record*, *245*(4), 708–714. https//doi.org/https://doi.org/10.1002/(SICI)1097-0185(199608)245:4<708::AID-AR11>3.0.CO;2-T

Calzada, N., Aguilar, A., Grau, E., & Lockyer, C. (1997). Patterns of growth and physical maturity in the western Mediterranean striped dolphin, *Stenella coeruleoalba* (Cetacea: Odontoceti). *Canadian Journal of Zoology*, *75*(4), 632–637, https://doi.org/10.1139/z97-078

Carlucci, R., Cipriano, G., Santacesaria, Francesca, C., Ricci, P., Maglietta, R., Petrella, A., Mazzariol, S., De Padovag, D., Mossag, M., Bellomo, S., & Fanizza, C. (2020). Exploring data from an individual stranding of a Cuvier's beaked whale in the Gulf of Taranto (Northern Ionian Sea, Central-eastern Mediterranean Sea). *Journal of Experimental Marine Biology and Ecology*, 533. https://doi.org/10.1016/j.jembe.2020.151473

Carlucci, R., Capezzuto, F., Cipriano, G., D'Onghia, G., Fanizza, C., Libralato, S., Maglietta, R., Maiorano, P., Sion, L., Tursi, A., & Ricci, P. (2021). Assessment of cetacean–fishery interactions in the marine food web of the Gulf of Taranto (northern Ionian Sea, central Mediterranean Sea). *Reviews in Fish Biology and Fisheries*, *31*, 135–156, https://doi.org/10.1007/s11160-020-09623-x

Carlucci, R., Ricci, P., Cipriano, G., & Fanizza, C. (2018a). Abundance, activity and critical habitat of the striped dolphin *Stenella coeruleoalba* in the Gulf of Taranto (northern Ionian Sea, central Mediterranean Sea). *Aquatic Conservation Marine and Freshwater Ecosystem*, *28*, 324–336, https://doi.org/10.1002/aqc.2867

Carlucci, R., Cipriano, G., Paoli, C., Ricci, P., Fanizza, C., Capezzuto, F., & Vassallo, P. (2018b). Random forest population modelling of striped and common bottlenose dolphins in the Gulf of Taranto (northern Ionian Sea, central-eastern Mediterranean Sea). *Estuarine Coastal Shelf Science*, *204*, 177–192, https://doi.org/10.1016/j.ecss.2018.02.034

Celli, J. P., Turner, B. S., Afdhal, N. H., Keates, S., Ghiran, I., Kelly, C. P., Ewoldt, R. H., McKinley, G. H., So, P., Erramilli, S., & Bansil, R. (2009). *Helicobacter pylori* moves through mucus by reducing mucin viscoelasticity. *Proceedings of the National Academy of Sciences of the United States of America*, *106*(34), 14321–14326. https://doi.org/10.1073/pnas.0903438106

Cornaglia, E., Rebora, L., Gili, C., & Di Guardo, G. (2000). Histopathological and immunohistochemical studies on cetaceans found stranded on the coast of Italy between 1990 and 1997. *Journal of Veterinary Medicine Series A*, *47*(3), 129–142. https://doi.org/10.1046/j.1439-0442.2000.00268.x

Cozzi, B., Huggenberger, S., & Oelschläger, H. (2017). Feeding and the digestive system. In B. Cozzi, S. Huggenberger, & H. Oelschläger (Eds.), *Anatomy of dolphins* (pp. 339–368). Academic Press. https://doi.org/10.1016/B978-0-12-407229-9.00008-7

Fayed, M. H., & Makita, T. (1997). Lectin histochemistry of the glandular part of the gastric mucosa of the one humped camel (*Camelus dromedarius*). *Acta histochemica et cytochemica*, *30*(5–6), 423–431. https://doi.org/10.1267/ahc.30.423

Gomez-Santos, L., Alonso, E., Diaz-Flores, L., Madrid, J. F., & Saez, F. J. (2018). Different glycoconjugate content in mucus secreting cells of the rat fundic gastric glands. *Anatomical Record*, *301*(12), 2128–2144. https://doi.org/10.1002/ar.23892

Harrison, R., Johnson, F., & Young, B. (1970). The oesophagus and stomach of dolphins (*Tursiops*, *Delphinus*, *Stenella*). *Journal of Zoology*, *160*(3), 377–390. https://doi.org/10.1111/j.1469-7998.1970.tb03088.x

Hosokawa, H., & Kamiya, T. (1971). Some observations on the cetacean stomachs, with special considerations on the feeding habits of whales. *Scientific Reports of the Whales Research Institute, Tokyo*, *23*, 91–101.

IJsseldijk, L. L., Brownlow, A. C., & Mazzariol, S. (2019). *Best practice on cetacean post mortem investigation and tissue sampling*. Joint ACCOBAMS and ASCOBANS Document. Istanbul. https://accobams.org/wp-content/uploads/2019/04/MOP7.Doc33_Best-practices-on-cetacean-post-mortem-investigation.pdf

Landini, G, Martinelli, G., & Piccinini, F. (2020). Colour deconvolution: stain unmixing in histological imaging. *Bioinformatics*, *37*(10), 1485–1487. https://doi.org/10.1093/bioinformatics/btaa847

Langer, P. (1996). Comparative anatomy of the stomach of the Cetacea. Ontogenetic changes involving gastric proportions - mesenteries - arteries. Zeitschrift für Säugetierkunde, *61*, 140–154.

Langer, P. (2017). *Comparative anatomy of the gastrointestinal tract in Eutheria II*. De Gruyter.

Liquori, G. E., Zizza, S., Mastrodonato, M., Scillitani, G., Calamita, G., & Ferri, D. (2005). Pepsinogen and H,K-ATPase mediate acid secretion in gastric glands of *Triturus carnifex* (Amphibia, Caudata). *Acta Histochemica*, *107*(2), 133–141. https://doi.org/10.1016/j.acthis.2005.03.002

Lueth, M., Sturegard, E., Sjunnesson, H., Wadstrom, T., & Schumacher, U. (2005). Lectin histochemistry of the gastric mucosa in normal and *Helicobacter pylori* infected guinea-pigs. *Journal of Molecular Histology*, *36*(1–2), 51–58. https://doi.org/10.1007/s10735-004-3838-2

Mastrodonato, M., Calamita, G., Rossi, R., Scillitani, G., Liquori, G. E., & Ferri, D. (2009). Expression of H^+,K^+-ATPase and glycopattern analysis in the gastric glands of *Rana esculenta*. *Journal of Histochemistry and Cytochemistry*, *57*(3), 215–225. https://doi.org/10.1369/jhc.2008.952234

Mastrodonato, M., Mentino, D., Liquori, G. E., & Ferri, D. (2013). Histochemical characterization of the sialic acid residues in mouse colon mucins. *Microscopy Research and Technique*, *76*(2), 156–162. https://doi.org/10.1002/jemt.22146

Mastrodonato, M., Mentino, D., Lopedota, A., Cutrignelli, A., & Scillitani, G. (2017). A histochemical approach to glycan diversity in the urothelium of pig urinary bladder. *Microscopy Research and Technique*, *80*(2), 239–249. https://doi.org/10.1002/jemt.22794

McCloy, R. A., Rogers, S., Caldon, C. E., Lorca, T., Castro, A., & Burgess, A. (2014). Partial inhibition of Cdk1 in G_2 phase overrides the SAC and decouples mitotic events. *Cell Cycle*, *13*(9), 1400–1412. https://doi.org/10.4161/cc.28401

McGowen, M. R. (2011). Toward the resolution of an explosive radiation—A multilocus phylogeny of oceanic dolphins (Delphinidae). *Molecular Phylogenetics and Evolution*, *60*(3), 345–357. https://doi.org/10.1016/j.ympev.2011.05.003

Mead, J. G. (2007). Stomach anatomy and use in defining systemic relationships of the cetacean family Ziphiidae (beaked whales). *Anatomical Record*, *290*(6), 581–595. https://doi.org/10.1002/ar.20536

Mentino, D., Mastrodonato, M., Rossi, R., & Scillitani, G. (2014). Histochemical and structural characterization of egg extracellular matrix in bufonid toads, *Bufo bufo* and *Bufotes balearicus*: Molecular diversity versus morphological uniformity. *Microscopy Research and Technique*, *77*(11), 910–917. https://doi.org/10.1002/jemt.22414

Milani, C., Vella, A., Vidoris, P., Christidis, A., Koutrakis, E., Frantzis, A., Miliou, A., & Kallianiotis, A. (2018). Cetacean stranding and diet analyses in the North Aegean Sea (Greece). *Journal of the Marine Biological Association of the United Kingdom*, *98*(5), 1011–1028. https://doi.org/10.1017/S0025315417000339

Ouwerkerk, J. P., de Vos, W. M., & Belzer, C. (2013). Glycobiome: bacteria and mucus at the epithelial interface. *Best Practice & Research Clinical Gastroenterology*, *27*(1), 25–38. https://doi.org/10.1016/j.bpg.2013.03.001

Petraccioli, A., Maio, N., Guarino, F. M., & Scillitani, G. (2013). Seasonal variation in glycoconjugates of the pedal glandular system of the rayed Mediterranean limpet, *Patella caerulea* (Gastropoda: Patellidae). *Zoology*, *116*(3), 186–196. https://doi.org/10.1016/j.zool.2012.10.006

Phillipson, M., Johansson, M. E. V., Henriksnas, J., Petersson, J., Gendler, S. J., Sandler, S., Persson, A. E. G., Hansson, G. C., & Holm, L. (2008). The gastric mucus layers: constituents and regulation of accumulation. *American Journal of Physiology-Gastrointestinal and Liver Physiology*, *295*(4), G806–G812. https://doi.org/10.1152/ajpgi.90252.2008

Rasband, W. (2016). ImageJ. U.S. National Institutes of Health. https://imagej.nih.gov/ij/

Ruifrok, A. C., & Johnston, D. A. (2001). Quantification of histochemical staining by color deconvolution. *Analytical and Quantitative Cytology and Histology*, *23*(4), 291–299.

Santhosh, S., Anandan, R., Sini, T. K., & Mathew, P. T. (2007). Protective effect of glucosamine against ibuprofen-induced peptic ulcer in rats. *Journal of Gastroenterology and Hepatology*, *22*(6), 949–953. https://doi.org/10.1111/j.1440-1746.2007.04840.x

Schumacher, U., Duku, M., Katoh, M., Jorns, J., & Krause, W. J. (2004). Histochemical similarities of mucins produced by Brunner's glands and pyloric glands: A comparative study. *Anatomical Record*, *278*(2), 540–550. https://doi.org/10.1002/ar.a.20046

Scillitani, G., & Mentino, D. (2015). Comparative glycopattern analysis of mucins in the Brunner's glands of the Guinea-pig and the house mouse (Rodentia). *Acta Histochemica*, *117*(7), 612–623. https://doi.org/10.1016/j.acthis.2015.06.003

Scillitani, G., Moramarco, A. M., Rossi, R., & Mastrodonato, M. (2011). Glycopattern analysis and structure of the egg extracellular matrix in the Apennine yellow-bellied toad, *Bombina pachypus* (Anura: Bombinatoridae). *Folia Histochemica et Cytobiologica*, *49*(2), 306–316. https://doi.org/10.5603/fhc.2011.0043

Scillitani, G., Zizza, S., Liquori, G. E., & Ferri, D. (2007). Lectin histochemistry of gastrointestinal glycoconjugates in the greater horseshoe bat, *Rhinolophus ferrumequinum* (Schreber, 1774). *Acta Histochemica*, *109*(5), 347–357. https://doi.org/10.1016/j.acthis.2007.02.010

Shimokawa, T., Doihara, T., Makara, M., Miyawaki, K., Nabeka, H., Wakisaka, H., Kobayashi, N., & Matsuda, S. (2012). Lectin binding pattern of gastric mucosa of Pacific white-sided dolphin, *Lagenorhynchus obliquidens*. *Journal of Veterinary Medical Science*, *74*(2), 155–160. https://doi.org/10.1292/jvms.11-0115

Slijper, E. J. (1962). *Whales*. Basic Books.

Smith, G. J. D. (1972). The stomach of the harbor porpoise *Phocoena phocoena* (L.). *Canadian Journal of Zoology*, *50*(12), 1611–1616. https://doi.org/10.1139/z72-212

Sommer, U., Rehn, B., & Kressin, M. (2001). Light and electron microscopic investigation of the lectin-binding pattern in the oxyntic gland region of bovine abomasum. *Annals of Anatomy*, *183*(2), 135–143. https://doi.org/10.1016/S0940-9602(01)80033-9

Tarpley, R. J., Sis, R. F., Albert, T. F., Dalton, L. M., & George, J. C. (1987). Observations on the anatomy of the stomach and duodenum of the bowhead whale, *Balaena mysticetus*. *American Journal of Anatomy*, *180*(3), 295–322. https://doi.org/10.1002/aja.1001800310

Wagner, C. E., Wheeler, K. M., & Ribbeck, K. (2018). Mucins and their role in shaping the functions of mucus barriers. *Annual Review of Cell and Developmental Biology*, *34*(1), 189–215. https://doi.org/10.1146/annurev-cellbio-100617-062818

Yamasaki, F., & Takahashi, K. (1971). Digestive tract of Ganges dolphin, *Platanista gangetica*. I. Oesophagus and stomach. *Okajimas Folia Anatomica Japonica*, *48*(5), 271–293. https://doi.org/10.2535/ofaj1936.48.5_271

Yamasaki, F., Takahashi, K., & Kamiya, T. (1974). Digestive tract of La Plata dolphin, *Pontoporia blainvillei*. I. Oesophagus and stomach. *Okajimas Folia Anatomica Japonica*, *51*(1), 29–51. https://doi.org/10.2535/ofaj1936.51.1_29

Zaiontz, C. (2019). *Real statistical analysis using Excel*. https://www.real-statistics.com

Zhou, K. Y., & Li, Y. M. (1981). On the intestine of baiji, *Lipotes vexillifer*. *Acta Zoologica Sinica*, *27*(3), 248–253.

How to cite this article: Carlucci, R., Cipriano, G., Fanizza, C., Gerussi, T., Maglietta, R., Petrella, A., Pietroluongo, G., Ricci, P., Semeraro, D., Guglielmi, M. V., Scillitani, G., & Mentino, D. (2021). Glycopatterns of the foregut in the striped dolphin *Stenella coeruleoalba*, Meyen 1833 from the Mediterranean Sea. *Marine Mammal Science*, 1–22. https://doi.org/10.1111/mms.12852